

# Synthesis and catalysis of nanometer-sized bimodal mesoporous aluminosilicate materials

Ye Zhang<sup>a,b,\*</sup>, Xi'e Shi<sup>a,c</sup>, Ji Man Kim<sup>b</sup>, Dong Wu<sup>a</sup>, Yuhan Sun<sup>a</sup>, Shaoyi Peng<sup>a</sup>

<sup>a</sup> *Institute of Coal Chemistry, Chinese Academy of Sciences, Taiyuan 030001, PR China*

<sup>b</sup> *Functional Materials Laboratory, Department of Molecular Science and Technology, Ajou University, Suwon 442-749, Republic of Korea*

<sup>c</sup> *Department of Chemistry, China East Normal University, Shanghai, PR China*

Available online 5 August 2004

## Abstract

Nanometer-sized (below 100 nm) bimodal mesoporous aluminosilicate molecular sieves (NBMAS) are obtained by using sol–gel method and cetyltrimethylammonium bromide (CTAB) as the structure-directing agent. Ordering-packed framework mesopore is created within the colloidal particles by the templating function of surfactant CTAB and disordered textual pore is formed by the aggregation of colloidal particles as an inter-particle pore. As a result of the special properties of the present material, the hydrothermal stability and catalytic life of the material is highly improved in the catalytic cracking reactions. ZSM-5, normal AlMCM-41 and amorphous alumina–silica with nanometer particle size were used in the catalytic cracking process for comparing purpose.

© 2004 Elsevier B.V. All rights reserved.

**Keywords:** NBMAS; Mesoporous; Sol–gel; Catalytic cracking

## 1. Introduction

Mobil researchers firstly reported the synthesis of pseudo-crystalline mesoporous material designated M41S in 1992 [1,2]. The mesoporous materials exhibit uniform pore sizes in the range of 2–10 nm as well as highly ordered mesostructures. When the reactants are too big to penetrate into the zeolite, mesoporous catalysts are very useful due to their large pore size compared with that of zeolite (<1 nm). For example, the substitution of Al for Si within the framework can generate the acid sites, and make the material being catalytically active in petroleum process especially for bulky molecules [3–5]. However, AlMCM-41 possesses long one-dimensional channel system that is not favorable for the molecular diffusion if its particle size is in micrometer scale. As a result, cumulated carbon species can be easily produced and deposited within the mesopores, which may reduce the catalytic life. Moreover, the hydrothermal stability of the MCM-41 is known to be too weak to use it for catalytic applications in the presence of water.

In the present work, nanometer-sized bimodal aluminosilicate molecular sieves (NBMAS) are synthesized and used as the catalyst for cracking of *n*-octane and 1,3,5-triisopropylbenzene, and the catalytic activity and hydrothermal stability are compared with those of normal AlMCM-41 and amorphous aluminosilicate material as well as ZSM-5 zeolite.

## 2. Experimental

### 2.1. Synthesis

The sol–gel synthesis of NBMAS can be referred to the literature [6]. Tetraethylorthosilicate (TEOS) and aluminum nitrate nonahydrate (ANN) were used as the silica and alumina source, respectively, in the presence of CTAB. The molar composition of the reaction mixture was as follows: 1.0 TEOS:0.13 ANN:40 H<sub>2</sub>O:8 C<sub>2</sub>H<sub>5</sub>OH:0.25 CTAB:10 NH<sub>4</sub>OH. The template was removed by calcination at 650 °C. AlMCM-41 and amorphous silica–alumina with the same Si/Al ratio was prepared through hydrothermal and sol–gel method, respectively. Ammonia was also used as the base catalyst.

\* Corresponding author. Tel.: +86 351 4069882;  
fax: +86 351 4041153.

E-mail address: [zhgye@yahoo.com](mailto:zhgye@yahoo.com) (Y. Zhang).

## 2.2. Structure and catalytic characterization

Nitrogen adsorption–desorption isotherms of samples were measured on an ASAP2000 apparatus at 77°K and their surface area and pore size distribution data were analyzed by BET method and BJH model, respectively. Solid-state  $^{27}\text{Al}$  MAS NMR experiments were conducted on an Infinityplus-400 spectrometer with resonance frequencies of 79.48°MHz. The catalytic cracking reaction of 1,3,5-triisopropylbenzene (TIPB) was carried out by pulse method. Catalyst of 60°mg and 0.2  $\mu\text{l}$  of reactants were used during each process. Blank experiments showed that there was no thermal cracking at the present reaction temperature. The cracking of *n*-octane was carried out on a continuous fixed-bed reactor at 400 °C and 2.0 MPa. Catalyst of 1.0 g was used for the reaction, and the flow rate of octane was determined as 0.06 ml/min. The hydrothermal treatment was conducted in 100% water steam at 800 °C for 2 h.

## 3. Results and discussion

### 3.1. Structure

The HRTEM image and pore size distribution of NBMAS prove that there are two kinds of pores, framework mesopore and textural pore, exist in the material [6] (see Figs. 1 and 2).

The ordering-packed framework mesopore is created by the templating function of the surfactant, which is similar but not very the same with the usual MCM-41 mesoporous molecular sieves [1]. The difference is that the length of the one-dimensional mesopore is much shorter than normal MCM-41 because of the smaller particle size as showed in Fig. 1, which is about 100 nm. It may be easier for the products to exit from the mesopore during the catalysis application process. The relatively larger pore at about 65 nm is considered as the inter-particle pore formed by

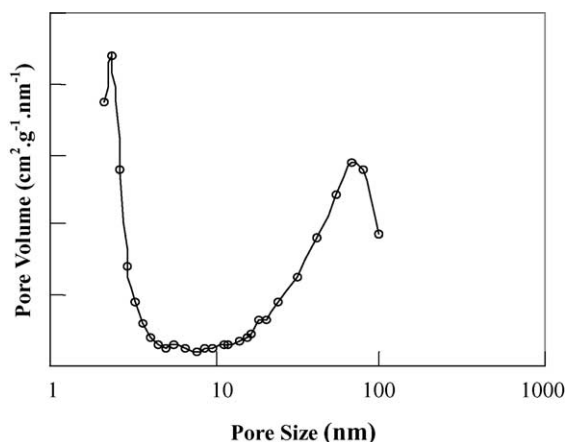


Fig. 2. Pore size distribution of NBMAS.

the aggregation of the colloidal particles during the sol–gel process. During the above synthesis, TEOS and ANN are firstly hydrolyzed in the neutral surfactant solution and formed aluminosilicate sols around the surfactant micelles because the higher concentration of water. Thus produced sols grow and aggregate quickly with each other at the same time as the concentrated ammonium catalyst is added once. Correspondingly, inter-particle pore (textural mesopore) is formed during the aggregation. While during the growth of nanoparticles around the surfactant micelle that acting as template, ordering-packed mesopore (framework mesopore) is formed as the usual synthesis mechanism of MCM-41. As a result, the material with bimodal mesopore structure is formed under present conditions. In addition, because the condensation rate of TEOS and ANN is limited by using the present sol–gel route comparing with the hydrothermal synthesis route, the growth of the nanoparticles is greatly controlled and as a result, nanoparticle-sized product is obtained. The detail structure information of NBMAS and MCM-41 as well as amorphous silica–alumina is listed in Table 1.

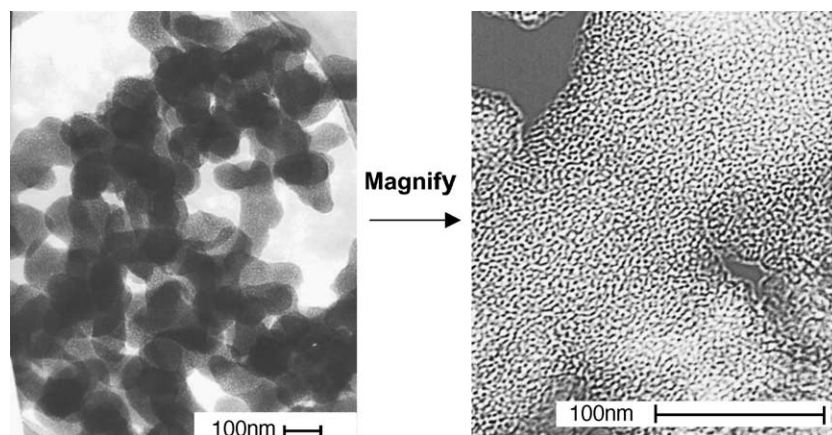


Fig. 1. HRTEM images of NBMAS.

Table 1  
The physical properties of NBMAS, MCM-41 and amorphous silica–alumina

Sample	$S_{\text{BET}}$ ( $\text{m}^2/\text{g}$ )	Pore size (nm)	Particle size (nm)
AIMCM-41	674	2.6	>700
NBMAS	513	2.42, 65.6	<100
Silica–alumina	149	75.8	<100

### 3.2. $^{27}\text{Al}$ MAS NMR characterization

The state of Al atoms in the sample is an important matter because octahedral extra framework Al species could be formed depending on the Al source used in the preparation or activation conditions [7,8]. Fig. 3 illustrates the  $^{27}\text{Al}$  MAS NMR spectra of the as-synthesized and calcined bimodal sample. It can be clearly observed that the as-synthesized material only exhibits one peak at about 53.0 ppm. No peak at 0 ppm corresponding to octahedral-coordinated Al species is detected, confirming that all of the Al atoms in the as-synthesized sample are present in a tetrahedral environment [9]. After calcinations, part of octahedral extra framework Al species and distorted tetrahedral Al species are produced which could be proved by the appearance of peaks at 24.7 and  $-4.6$  ppm in the  $^{27}\text{Al}$  MAS NMR spectra of the calcined sample. The Si/Al ratio of calcined samples is determined by chemical element analysis and the ratio (8.51) is a little higher than that of the starting material (7.5) because of the incorporation of Al atoms into the structure is less favored than Si species as well as the dealumination during calcination.

### 3.3. Acidity

The acidity of the samples is characterized by temperature-programmed desorption of ammonia ( $\text{NH}_3$ -TPD) in Fig. 4. Obviously, there are two kinds of acid in all of the samples, i.e., weak acid and middle strong acid. From the figure we can indicate that the samples possessed different amount of available acids because of their different structure although they possess the same Si/Al ratio. NBMAS possesses the largest amount of available weak acidity among the three samples and this can be attributed to the

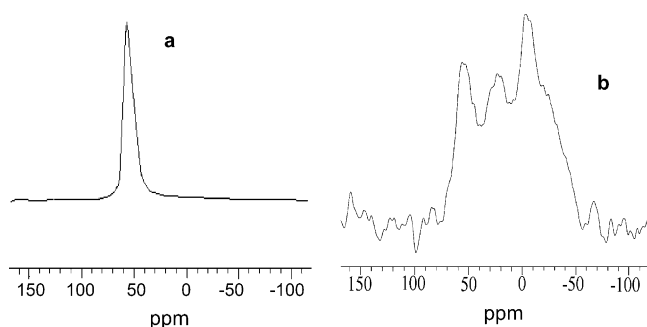


Fig. 3.  $^{27}\text{Al}$  MAS NMR spectra of the as-synthesized (a) and calcined (b) NBMAS.

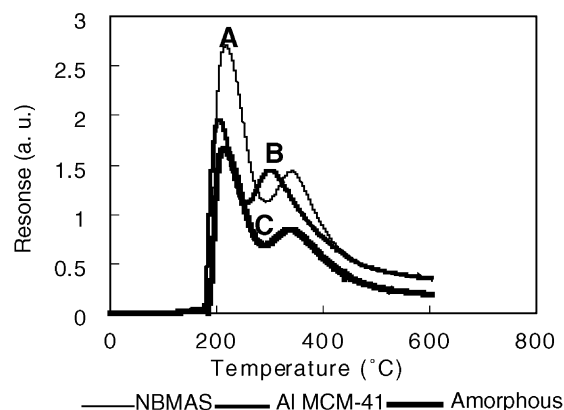


Fig. 4.  $\text{NH}_3$ -TPD curves of the samples of (A) NBMAS, (B) AIMCM-41 and (C) amorphous silica–alumina materials.

smaller particle size than AIMCM-41 and the creation of ordering-packed mesopore within the colloidal particles of amorphous silica–alumina material that improved the available acid sites for NBMAS. In addition, the intensity of the middle strong acid is a little stronger (at higher desorption temperature) for NBMAS and amorphous material than AIMCM-41, this may results from the sol–gel synthesis technology which leading to the nanometer particle size.

### 3.4. Catalytic cracking of *n*-octane

The reaction was carried out on a continuous fixed-bed and the products were collected and analyzed per hour. Table 2 lists the octane conversion and cracking selectivity results obtained at the second hour. As shown in Table 2, NBMAS shows higher catalytic activity and cracking selectivity than AIMCM-41 and amorphous silica–alumina. The creating of shorter ordering-packed mesopore within NBMAS improves its acid sites and at the same time performed more in favorite for the exiting of product molecules. Furthermore, the catalytic activity of AIMCM-41 decreased greatly (from 10.53% to 3.18%) after the reaction conducted on for about 3 h. While for NBMAS and the amorphous material, high catalytic activity is still remained even after 5 h. The shorter one-dimensional pore promotes the products exiting from the pore and in turn reduces the formation of cumulated carbon, which prolongs the life of catalyst.

### 3.5. Catalytic cracking of 1,3,5-triisopropylbenzene

ZSM-5 has been found widespread application as a fluid catalytic cracking additive for both propylene production and

Table 2  
The catalytic cracking of *n*-octane on different material

Sample	Conversion of C8 (%)	Cracking percent (%)
AIMCM-41	10.53	93.1
NBMAS	19.57	96.8
Silica–alumina	13.32	87.6

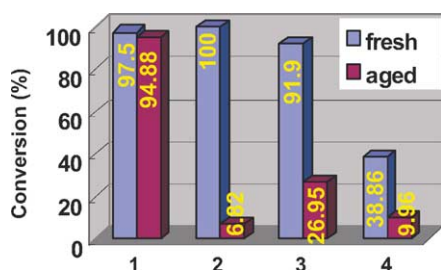


Fig. 5. Conversion of TIPB on different catalyst (1: NBMAS; 2: MCM-41; 3: amorphous SiO<sub>2</sub>-Al<sub>2</sub>O<sub>3</sub>; 4: ZSM-5). The age is carried out at 800 °C in 100% steam for 2 h.

gasoline octane improvement [10]. In addition, it was also realized that ZSM-5 accumulated coke much more slowly than the base Y zeolite cracking catalyst with which it was combined [11]. So we choose ZSM-5 as the comparing zeolite catalyst and it is proved to possess the micropore at 0.45 nm. Triisopropylbenzene is used as the catalytic cracking precursor because its molecular dynamic diameter is about 0.94 nm, which is larger than the pore size of usual microporous zeolites and smaller than mesoporous molecular sieves.

The conversion of TIPB at 300 °C on different catalyst before and after hydrothermal treatment at 800 °C in 100% steam is showed in Fig. 5. For the fresh samples, NBMAS, MCM-41 and amorphous silica–alumina all show high catalytic activity (above 90%) because of the high aluminum content and large pore size into which TIPB can easily enter [12]. But for ZSM-5, the conversion is much lower even on the fresh catalyst and this is mainly because the limited pore size (0.45 nm) of ZSM-5. Most of the active sites of ZSM-5 cannot be contacted fully by the reactant and the catalytic cracking is only processed on the surface of catalyst. As a result, the conversion of TIPB is greatly decreased.

Although the catalytic activity of fresh NBMAS, MCM-41 and amorphous silica–alumina are similar, the aged materials show great difference for the cracking of TIPB. After the strict hydrothermal treatment in 100% steam at 800 °C, the activity of MCM-41 and amorphous silica–alumina decreases very much and nearly disappears for MCM-41. The structure collapses and most of the framework aluminum is destroyed by the hydrothermal treatment. The surface area decreases from 674 to 25 m<sup>2</sup>/g and the pore volume decreases from 0.7 to 0.077 cm<sup>3</sup>/g, i.e., nearly all the mesostructure collapse. Although the present amorphous silica–alumina material also has a nanometer particle size, the framework aluminum is still not stable enough to endure the hot steam. While, the conversion of TIPB on aged NBMAS is still very high. It still remains some surface area (from 513 to 205 m<sup>2</sup>/g) and pore volume (from 0.465 to 0.195 cm<sup>3</sup>/g). The combination of nanometer particle size and dual porosity may lead to the simul-

taneously high hydrothermal stability and high catalytic activity.

#### 4. Conclusions

Mesoporous aluminosilicate materials with adjustable pore structure and particle size are synthesized via sol–gel route. Nanometer bimodal mesoporous aluminosilicate molecular sieves can be obtained by carefully controlling of the sol–gel process. The two kinds of pores are respectively formed by the templating function of surfactant and the aggregation of colloidal particles which are proved by XRD and HRTEM analysis. At the same time, the state of Al atoms in the as-synthesized sample are presented in a tetrahedral environment that introduced by the present sol–gel route. NBMAS shows higher catalytic activity and longer catalysis life on the cracking of *n*-octane and 1,3,5-triisopropylbenzene in comparing with AIMCM-41 and amorphous silica–alumina materials. The shorter one-dimensional mesopore and the relative larger pore promote the diffusion of reactant and product molecules to access and exit the pores. As a result, cumulated carbon is reduced and NBMAS perform longer catalytic life than normal AIMCM-41.

#### Acknowledgements

The authors would like to thank the National Key Basic Research Special Foundation (G2000048001) and Brain Korea 21 Project as well as Shanxi Youth Foundation (20041012) for the financial support.

#### References

- [1] C.T. Kresge, M.E. Leonowicz, W.J. Roth, J.C. Vartuli, J.S. Beck, *Nature* 359 (1992) 71.
- [2] J.S. Beck, J.C. Vartuli, W.J. Roth, M.E. Leonowicz, et al., *J. Am. Chem. Soc.* 114 (1992) 10834.
- [3] Y. Han, F.-S. Xiao, S. Wu, Y. Sun, X. Meng, D. Li, S. Lin, *J. Phys. Chem. B* 105 (2001) 7963.
- [4] D.Y. Zhao, C. Nie, Y.M. Zhou, S.J. Xia, L.M. Huang, Q.Z. Li, *Catal. Today* 68 (2001) 11.
- [5] J. Weglarski, J. Datka, H.Y. He, J. Klinowski, *J. Chem. Soc., Faraday Trans.* 91 (1995) 2995.
- [6] Y. Zhang, D. Wu, Y. Sun, S. Peng, et al., *Stud. Surf. Sci. Technol.* 146 (2003) 161.
- [7] Z. Luan, C.F. Cheng, H. He, J. Klinowski, *J. Phys. Chem.* 99 (1995) 1018.
- [8] M. Janicke, D. Kumar, G.D. Stucky, B.F. Chmelka, *Stud. Surf. Sci. Catal.* 84 (1994) 243.
- [9] C.Y. Chen, H.X. Li, M. Davis, *Micropor. Mater.* 2 (1993) 17.
- [10] T.F. Degnan, G.K. Chitnis, P.H. Schipper, *Micropor. Mesopor. Mater.* 35–36 (2000) 245–252.
- [11] L.D. Rollmann, D.E. Walsh, *J. Catal.* 56 (1979) 139.
- [12] H. Koch, W. Reschetilowski, *Micropor. Mesopor. Mater.* 25 (1998) 127.